NURETH14-94

NUMERICAL ASSESSMENT OF PANDA EXPERIMENTS COVERING STEAM/AIR/HELIUM MIXTURES

Namane Méchitoua, Stéphane Mimouni

Electricité de France R&D Division 6, Quai Watier, 78400 Chatou Cedex France namane.mechitoua@edf.fr, stephane.mimouni@edf.fr

Abstract

The accurate modeling of gas distribution (air, steam and Hydrogen) in a PWR containment, which are released after the beginning of a severe accident leading to the melting of the core, concerns phenomena such as wall condensation, hydrogen accumulation, gas stratification and transport in the different compartments of the containment. The paper presents numerical assessments of the test 25 of the PANDA experiment, using a homogeneous approach with the in-house CFD solver *Code_Saturne*. The paper is focused on the analysis and understanding of gas stratification and complex transport phenomena involved in such configurations.

1. Introduction

A severe accident in a PWR nuclear power plant generally originates from a lack of cooling of the core, whose residual power can no longer be evacuated. In a few hours, due to multiple failures, human or hardware, including the failure of backup procedures, the structure of fuel elements deteriorates. Hydrogen is produced from the oxidation of zirconium clads and of structures of fuel elements during the phase of core degradation.

The hydrogen and steam thus produced are transferred to the containment and then transported by convection loops. Given the significant differences in density between hydrogen and other gases in the containment (nitrogen, oxygen, water vapor, carbon monoxide, carbon dioxide, ...), hydrogen can accumulate preferentially in the upper parts of the compartments of the reactor building. In case of strong heterogeneity, hydrogen can achieve high local concentrations that exceed the threshold flammable gas mixture and lead to fast combustion.

Among the different safety systems for limiting the pressure increase during the course of the accident and the impact of possible fast combustion, European PWR reactors use two types of mitigation means:

- The passive auto-catalytic recombiners (PAR): their role is to reduce the amount of hydrogen by means of a catalytic reaction, oxidizing hydrogen to steam and to generate a buoyancy (chimney) flow that mixes the containment atmosphere.
- Spray systems: the injected water droplets cool the containment and decrease the pressure by condensing steam on the droplets. They also promote mixing of gas by breaking quickly possible stratifications of the lightest gases.

The walls of the containment building and metallic structures play an important role from a thermal viewpoint. The walls, initially colder than the gas, condense the water vapor contained in the gas mixture and thus limit the pressure increase in the containment. Furthermore, the temperature

difference between fluid and walls generates convection loops, enhancing the mixing of gases having different density.

This paper focuses on numerical assessments of gas transport and stratification phenomena with CFD solver *Code_Saturne* [1], [2] and CMFD solver NEPTUNE_CFD [3], [4]. It is organized as follows. The first part describes the homogeneous gas dynamic model implemented in *Code_Saturne*. As the multi-fluid model of NEPTUNE_CFD has already been presented several times [5], [6], [7], it is not described here. The second part concerns the numerical assessments with *Code_Saturne* upon the test n° 25 of the PANDA experiment, performed at PSI [8] in the frame of OECD/SETH project.

2. Homogeneous Gas Dynamic Model used in Code Saturne

The motion of gases and heat transfer in containment enclosures can be described by the general momentum, partial masses and energy conservation equations [9]. The predominant physical phenomena driving the distribution and heat transfer of fluids are the following:

- Mixing and /or segregation of gas whose velocity, density and temperature are different.
- Pressurization of containment: the compressibility of gas is taken into account, even if the flow velocities are low when compared to the acoustic speed.
- Catalytic reaction in recombiners, in order to limit Hydrogen concentration.
- Condensation of steam on cold structure surfaces, which limits the pressure rise in the containment.

The general momentum, partial masses and energy conservation equations describing these phenomena can be simplified and stiffness due to the presence of physics having very different characteristic length and time scales can be removed or relaxed.

The model is based on a low Mach number approximation, with a standard k-ε model for turbulence. Fluid-structure heat transfers are modeled through wall log laws and Chilton-Colburn correlations.

2.1 Low mach number approximation

The flows are mainly low Mach number flows, whose motion is predominantly driven by free convection. A low Mach number model can be implemented within a pressure correction based solver usually used for incompressible or steady dilatable flows, as $Code_Saturne$ [2]. A spatial filtering of acoustic waves leads to the separation of the static pressure P into a uniform time-dependent thermodynamic pressure $P_{th}(t)$ and a mechanical pressure p(x,t) [10]:

$$P = P_{th}(t) + p(x,t); \ P_{th} >> |p(x,t)|$$
 (1)

The general motion conservation equation of the mixture

$$\frac{\partial \rho \vec{U}}{\partial t} + div[\vec{U} \otimes \rho \vec{U} - \mu_{tot}(\vec{\nabla} \vec{U} + {}^t \vec{\nabla} \vec{U}) + (2/3 \mu_{tot} div \vec{U} + 2/3 \rho k + P)\vec{1}] = \rho \vec{g} + \Gamma_{cond} \vec{U}_I$$

associated with supplementary approximations concerning the mechanical pressure and the taking into account of mean hydrostatic pressure as

$$p(x,t) = p(x,t) + 2/3 \,\mu_{tot} \operatorname{div} \vec{U} + 2/3 \rho \,k + \rho_0 \,g \,z \text{ with } \rho_0 \equiv \int \rho d\Omega / \Omega_0$$

then becomes:

$$\frac{\partial \rho \vec{U}}{\partial t} + div[\vec{U} \otimes \rho \vec{U} - \mu_{tot}(\vec{\nabla} \vec{U} + \vec{\nabla} \vec{U})] + \vec{\nabla} p = (\rho - \rho_0)\vec{g} + \Gamma_{cond}\vec{U}$$
(2)

where ρ , U, μ_{tot} , p, ρ_0 , \mathbf{g} and Γ_{cond} stand respectively for the mixture density, the mixture velocity vector, the total dynamic viscosity (including the turbulent viscosity deduced from the k- ϵ turbulence

model), the mechanical pressure, the averaged density, the gravity acceleration and the condensation sink term. Thanks to the low Mach number approximation (1), the mechanical pressure is neglected for the computation of density, through the thermal equation of state:

$$\rho = \frac{P_{th}}{RT\sum_{k} \frac{Y_{k}}{M_{k}}} \tag{3}$$

where R, T, Y_k and M_k stand respectively for the perfect gas Constant, the absolute temperature (in Kelvin), the mass fractions of the different gases contained in the reactor building during a severe accident (Oxygen, Nitrogen, Steam and Hydrogen).

The additional unknown P_{th} is solved, using integral forms over the entire domain Ω_0 of mass or enthalpy equations, written below:

$$\frac{\partial}{\partial t} \int_{\Omega_{0}} \rho \, d\Omega = \int_{\Omega_{0}} \Gamma_{\text{cond}} \, d\Omega - \int_{\partial\Omega_{0}} \rho \, \vec{U} \, \vec{n} \, dS$$
or
$$\frac{dP_{th}}{dt} \Omega_{0} = -\frac{\partial}{\partial t} \int_{\Omega_{0}} \rho \, h \, d\Omega - \int_{\partial\Omega_{0}} \left[\rho \, \vec{U} \, h - \left(\frac{\mu_{t}}{\sigma_{t}} + \frac{\lambda}{C_{p}} \right) \vec{\nabla} h \right] \, \vec{n} \, dS + \int_{\Omega_{0}} \rho \, S_{h} \, d\Omega$$
(4)

2.2 Energy equation

The enthalpy equation of the mixture is quite complex and contains several terms. The body forces, the viscous constraint contributions, the supplementary terms due to the presence of more than two different species are negligible, when compared to the convective and turbulent transport contributions. For low Mach number flows, the kinetic energy remains small when compared to the thermal energy. On the other side, the unsteady contribution of the thermodynamic pressure is conserved, as it plays a key role in the pressure rise in the containment.

The Fourier laminar and turbulent conduction term is directly written according to the enthalpy variable through the following linearization: $\lambda \frac{\partial T}{\partial x_j} = \frac{\lambda}{C_p} \frac{\partial h}{\partial x_j}$,

where λ and C_p stand respectively for conductivity and specific heat of the gas mixture. The enthalpy equation is finally written in the following form:

$$\frac{\partial \rho h}{\partial t} + div \left[\rho \vec{U} h - \left(\frac{\mu_t}{\sigma_t} + \frac{\lambda}{C_n} \right) \vec{\nabla} h \right] = \frac{dP_{th}}{dt} + \Gamma_{cond} h_{steam} - \rho \cdot E \cdot \dot{w}_{H2}$$
 (5)

where h stands for the sensitive enthalpy of the gas mixture, defined as $h = \int_{T_0}^{T} C_p dT$.

Then, in presence of exothermic chemical reactions, due to the combustion of hydrogen by the recombiners, the transformation of formation enthalpy into sensitive enthalpy is taken into account through a source term proportional to the reaction heat E released by the chemical reactions and to the chemical reaction speed $w_{\rm H2}$.

We recall that the formation enthalpies and reaction heat E of Hydrogen at ambient temperature are : $h_{H_2}^0(T_0) = h_{H_2}^0(T_0) = h_{O_2}^0(T_0) = h_{N_2}^0(T_0) = 0$; $h_{H_2O,vap}^0(T_0) = -13.4 \, MJ/kg$ E = 1.22 MJ/kg

The heat transfer due to condensation at the walls is modeled through a sink term proportional to the steam mass reduced into liquid water Γ_{cond} and the latent heat L_{cond} (~2.44 MJ/kg).

2.3 Mass conservation equations

The mass conservation equations are written as below:

- the global mass equation, containing the sink term of wall condensation:

$$\frac{\partial \rho}{\partial t} + div(\rho \vec{U}) = \Gamma_{cond} \tag{6}$$

- the conservation equations of non condensable gases, containing the slow combustion sink terms due to the recombiners:

$$\frac{\partial \rho Y_{O2}}{\partial t} + \operatorname{div}(\rho \vec{U} Y_{O2} - \rho D \vec{\nabla} Y_{O2}) = \Gamma_{O2} = \rho \frac{M_{O2}}{2 M_{H2}} \dot{w}_{H2}
\frac{\partial \rho Y_{H2}}{\partial t} + \operatorname{div}(\rho \vec{U} Y_{H2} - \rho D \vec{\nabla} Y_{H2}) = \Gamma_{H2} = \rho \dot{w}_{H2}
\frac{\partial \rho Y_{N2}}{\partial t} + \operatorname{div}(\rho \vec{U} Y_{N2} - \rho D \vec{\nabla} Y_{N2}) = \Gamma_{N2} = 0$$
(7)

- the relation for obtaining the condensable gas (steam) from the concentration of the other gases:

$$Y_{H2O} = 1 - Y_{O2} - Y_{N2} - Y_{H2} \tag{8}$$

2.4 Turbulence Modeling

The standard k- ε turbulence model, adapted to the variable density flows, is used. The equations of the kinetic energy k and the turbulence dissipation ε obtained by a Favre averaging are as follows:

$$\frac{\partial \rho \, k}{\partial t} + \operatorname{div}(\rho \, \vec{U} \, k \, - \frac{\mu_t}{\sigma_t} \, \vec{\nabla} k) = P + G - \rho \, \varepsilon \tag{9}$$

$$\frac{\partial \rho \, \varepsilon}{\partial t} + div(\rho \, \vec{U} \, \varepsilon \, - \frac{\mu_t}{\sigma_{\varepsilon}} \, \vec{\nabla} \varepsilon) = C_{\varepsilon 1} \, \frac{\varepsilon}{k} \Big[P + (1 - C_{\varepsilon 3}) G \, \Big] - C_{\varepsilon 2} \rho \, \frac{\varepsilon^2}{k}$$

$$\tag{10}$$

where P and G represent respectively the contribution to the turbulence production of the inertia and of the buoyancy forces:

$$P = 2\mu_t tr \left[\left(\vec{\nabla} \vec{U} + \vec{\nabla} \vec{U} \right)^2 \right] - \frac{2}{3} \rho k \operatorname{div} \vec{U} - \frac{2}{3} \mu_t (\operatorname{div} \vec{U})^2 \quad , \quad G = -\frac{\mu_t}{\sigma_t} \vec{g} \frac{\vec{\nabla} \rho}{\rho}$$

$$\tag{11}$$

Then, the turbulent viscosity is given as:
$$\mu_t = C_{\mu} \rho \frac{k^2}{\epsilon}$$
 (12)

The constants of the model are given by [11] and are as follow:

$\sigma_{\rm t}$	σ_{ϵ}	σ_{k}	C_{μ}	$C_{\epsilon 1}$	$C_{\epsilon 2}$	$C_{\varepsilon 3}$
0.9	1.3	1	0.09	1.44	1.92	1 if G<0, 0 if G>0

2.5 Wall condensation modeling

Steam condensation on the walls of the containment enclosure plays a key role in the dynamic and heat transfer. The heat and mass sink terms of gases due to condensation are modeled through correlations based on heat and mass transfer analogy, of Chilton-Colburn type [12]. The liquid film is not modeled and it is assumed that vapor and non condensable gases are in direct contact with the wall. The heat transfer by condensation of steam in liquid is written as:

$$\phi_{cond} = \dot{m} L_{cond} \tag{13}$$

where \dot{m} and L_{cond} (~2.44 MJ/kg) represent respectively the mass per unit time of steam condensed in liquid and the latent heat between liquid water and steam.

The analogy with the Chilton-Colburn correlation is used for modeling the mass transfer:

$$\dot{m} = \frac{\rho D_{inc/vap}}{z} Sh_z \frac{Y_i - Y}{Y_i} \tag{14}$$

where:

- D_{inc/vap} is the molecular diffusion coefficient between steam and non condensable gases.
- Y_i an Y are the mass fractions of the non condensable gases respectively at the liquid/gas interface and far from the interface (in fact, in the cell adjacent to the cold wall).
- Sh_z is the Sherwood number based on the distance z is the length of the boundary layer

The interface non condensable gases mass fraction is deduced from the molar fraction, which depends on the thermodynamic pressure P_{th} and the steam saturation pressure P_{H2Oi} .

$$X_{i} = 1 - X_{H2O,i} = 1 - P_{H2O,i} / P_{th} = 1 - P_{sat} / P_{th}$$

The Sherwood number depends on local Reynolds and Grashoff numbers, defined as below.

$$Sh_{z} = \xi \max [0.029Re_{z}^{4/5} Sc^{1/3}, 0.13(Gr_{z}Sc)^{1/3}]$$
with $\xi = 1 + 0.625 \frac{X_{i} - X}{X_{i}}$, $Re_{z} = \frac{Uz}{v}$, $Gr_{z} = \frac{g(\delta \rho / \rho)z^{3}}{v^{2}}$ and $\delta \rho = |\rho(T_{i}, Y_{i}) - \rho(T, Y)|$

For buoyancy dominated flows, the Sherwood number mainly depends upon the Grashoff number. Then, the correlation is independent of z, the length of the boundary layer.

2.6 Wall temperature modeling

The long term mixing phenomena in the containment are closely related to the heat and mass transfer due to the condensation of steam in contact with colder structures. Then, it depends on the wall temperatures, which evolves in function of unsteady heat conduction. The use of a one dimensional unsteady formulation approach gives enough precision, because the unsteady behavior of wall temperature depends much stronger on the condensation and gaseous heat fluxes than on the transverse heat conduction.

The boundary conditions of this computation are given by the following conditions:

- equation (13) for the heat transfer due to condensation and a mixed log law/ Chilton-Colburn correlation for heat transfer in gaseous phase,
- an external condition, taking into account the presence or not of insulation and the external temperature.

2.7 Numerical Procedure

A numerical procedure based on a segregated approach of SIMPLE type is used for advancing in time [3], [2]. The first step consists of predicting the velocity field from the momentum equations. This step solves an implicit equation for velocity, all other variables as pressure being frozen. Then, a reduced form of the momentum equation containing the predicted velocity and the implicit part of the mechanical pressure is coupled with the global mass equation. The mass accumulation term verifying the global conservation (4) is taken into account in the right hand side of the mechanical pressure equation. A strong conservative form of all transport equations according to the time and spatial derivatives is preferred to a volumetric form of the mass equation used for fire simulations [13]. The volumetric form of mass equation is more precise for coarse discretization for which the mesh Reynolds number is high, but this formulation can be too sensitive to loss or gain of mass for long transient simulation within closed containment, as it is the case for safety studies concerning nuclear severe accidents.

Spatial discretization follows a 3D full unstructured finite volume approach, with a collocated arrangement of all variables. A face based data structure allows the use of arbitrary shaped cells, including non matching meshes. Numerical consistency and precision for diffusive and convective fluxes for non orthogonal mesh and irregular cells are taken into account through a gradient reconstruction technique and non linear schemes. Only the "dynamic" part of the pressure gradient is concerned by this stabilization technique, as an a priori evaluation of the "hydrostatic" part is performed before solving the momentum equations.

2 PANDA test 25 simulations

The PANDA experiments performed at PSI [8] provide data of 3D gas flow and distribution issues in both PWR and BWR containments. The addressed phenomena play a key role for code prediction capability improvements, accident management and design of mitigating measures. The experiments are conducted at large scale in a multi-compartment geometry for providing data suitable for improvement and validation of safety analysis codes.

The PANDA experiment represents containment compartments and the Reactor Pressure Vessel by six cylindrical pressure vessels. The total height of the facility is 25 m, the total volume of the vessels is about 460 m³ and the maximum operating conditions are 10 bars and 200°C. For the SETH tests concerning local investigations of flows, only some parts of the facility are used. Experiments are carried out in a large volume of about 180 m³ consisting of two identical vessels, 8 m in height and 4 m in diameter. Figure 1 represents the part of PANDA facility which has been simulated (drywells DW1 and DW2 only). The connection between DW1 and the Wetwell is modeled through an inlet/ outlet free boundary condition with an imposed mechanical pressure and extrapolation conditions for all other variables if the flow is entering. As the meshes used are relatively coarse (corresponding to an engineering use), the injection of gases in DW1 are modeled through source terms representing exactly momentum, energy and mass gases flow-rates.

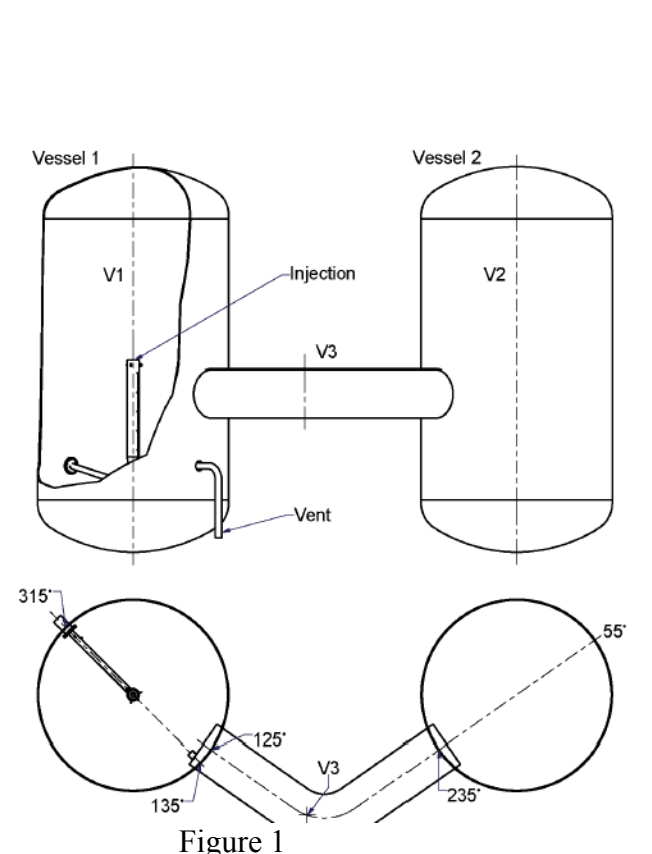
The 14th International Topical Meeting on Nuclear Reactor Thermalhydraulics, NURETH-14 Toronto, Ontario, Canada, September 25-30, 2011

The initial conditions and the scenario schedule are the following:

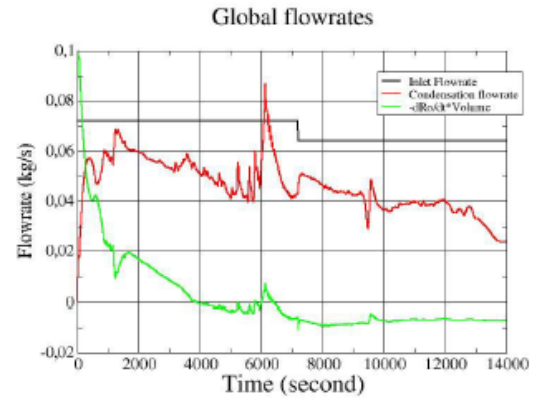
Pressure=1.3 bars; Fluid and Structure temperature=27°C, Gas composition: Air only.

Scenario Schedule (second)	0 up to 7,200	7200 up to 14,400
Linear pressure increase (bars)	1.3 up to 2.6	2.6 up to 3.0
Injection Fluid Temperature (°C)	120	150
Helium Flow rate (kg/s)	0.008	0.000
Steam Flow rate (kg/s)	0.064	0.064

Figure 2 shows the different global flow-rates and mass balances of Steam, Helium and Air contained in drywells DW1 and DW2 and the interconnecting pipe obtained with the structured intermediate mesh of 28,000 cells. Although the mesh independency is not yet achieved, this intermediate mesh gives acceptable results for a physical analysis. The mass accumulation term significantly decreases at the beginning of the scenario. Then, after 4000 seconds, this term stabilizes to a lower value, which corresponds to an increase of mass in the two vessels. At the end, the mass is about the same that at the beginning of the transient. The condensation flow-rate is very important and nearly corresponds to 2/3 of the injected steam. The mass decreases at the beginning because the lightest fluid as helium and steam replaces the heaviest fluid as air. The slightly increase in pressure smoothes this decrease. The Helium and steam masses both increase during the first part of the transient. Then, the mass of helium slightly decreases (no injection of this gas during the second part of the transient) and this gas is replaced by steam (increase in steam mass stronger than that during the first part of the scenario).



PANDA facility configuration for the SETH Three Gas Mixtures test 25



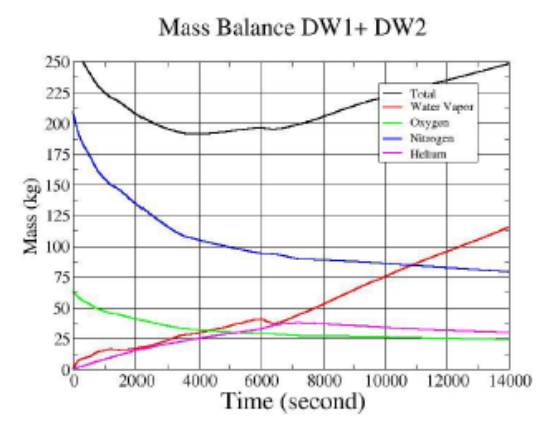


Figure 2
Global mass balance in DW1+ DW2
during the simulated scenario.

Figure 3 shows snapshots of helium volume fractions in the vertical symmetry plane of the two vessels. The beginning of the transient is driven by positive buoyancy effects, for which the lightest fluid as Helium rises rapidly in the upper part of the two vessels. Then, as steam is condensed upon the cold structures surrounding the gases, the helium concentration in the first vessel relatively increases according to the other gases and fluid become lighter than the injected fluid mainly composed of steam. A negative buoyancy effect is then observed, for which the injected fluid falls down in the first vessel, as it can be seen in the 3rd and 4th snapshot. The sedimentation of the fluid in the first vessel is observed a short time after the beginning of the transient.

Figure 4 compares some experimental data with numerical results. It concerns the volume fractions of gases at the vent and at three positions along a vertical line in the two vessels (dome, middle and low). The first figure shows the unsteady behavior of the different gases (air, helium and steam) at the vent. The stratification is eroded slightly earlier, when compared to other numerical results [15], [16]. We observe the arrival of Helium and steam too early. At the end of the transient, the numerical curves join the experimental curves, indicating a good behavior of the condensation model and the global conservation in time and space of the numerical model.

The second figure shows the helium volume concentration with respect to the time at 3 spatial levels in the first vessel. The lowest level, below the vent, is not well predicted, indicating a too early arrival of helium and steam. This behavior is also reproduced by other flow solvers [15], [16]. At the end of the transient, the numerical results compare well with experimental data.

The last figure 4 shows the obtained results in the second vessel. The simulations reproduce much better the experimental behavior, when compared to the numerical results obtained for the first vessel. The flow in this vessel, much less perturbed than in the first vessel, is mainly driven by positive buoyancy leading to stratifications. The stratifications of dominantly helium gas in the upper parts and of a mixture of air, helium and steam in the intermediate part, at the level of the interconnecting pipe remain quite stable for a transient of about 14,000 seconds. Besides, the stratification of dominantly air gas in the lowest part is slowly eroded by the arrival of helium and steam from the upper levels of the vessel. Indeed, the helium volume concentration continuously rises from 0 to 0.2 for a duration of about 10,000 seconds, as it is shown as well as by experimental data that by numerical simulations.

Figure 5 shows the transient of fluid temperature at 4 locations in the first vessel (DW1) computed with different time steps and the comparison with available experimental data. The main trends of the temperature behavior, as well as in term of levels that in term of unsteady behavior, are captured by the numerical model. Nevertheless, the computed temperatures are slightly over-estimated at the beginning of the transient, indicating that the characteristic time of the condensation model based on an analogy with Chilton-Colburn correlation is probably too large.

Figure 6 shows the internal structure temperature (time 14,400 seconds) obtained by an unsteady one dimensional heat conduction model, applied to the 2 cm large steel structure of the vessels DW1 and DW2, insulated by 20 cm of rock-wool. The stratification and sedimentation phenomena within the fluid strongly influenced the structure temperature. The highest level of structure temperatures at the end of the transient are located at the intermediate and lower part of DW1 vessel, where mixing phenomena between air, steam and helium due to sedimentation of the fluid enhances heat transfer between the fluid and the structures. The lowest level of structure temperature at the end of the transient are located at the upper parts of DW1 and DW2 vessels and at the lower part of DW2 vessels. The presence of light Helium gas stratification in the upper part and heavy air gas in the lower part block the arrival of hot steam gas and prevent mixtures and the structure temperature increase. The transient of the structure temperature at three levels (dome, intermediate, low) in the first vessel is correctly predicted and is comparable to the results obtained by other flow solvers [15].

The 14th International Topical Meeting on Nuclear Reactor Thermalhydraulics, NURETH-14 Toronto, Ontario, Canada, September 25-30, 2011

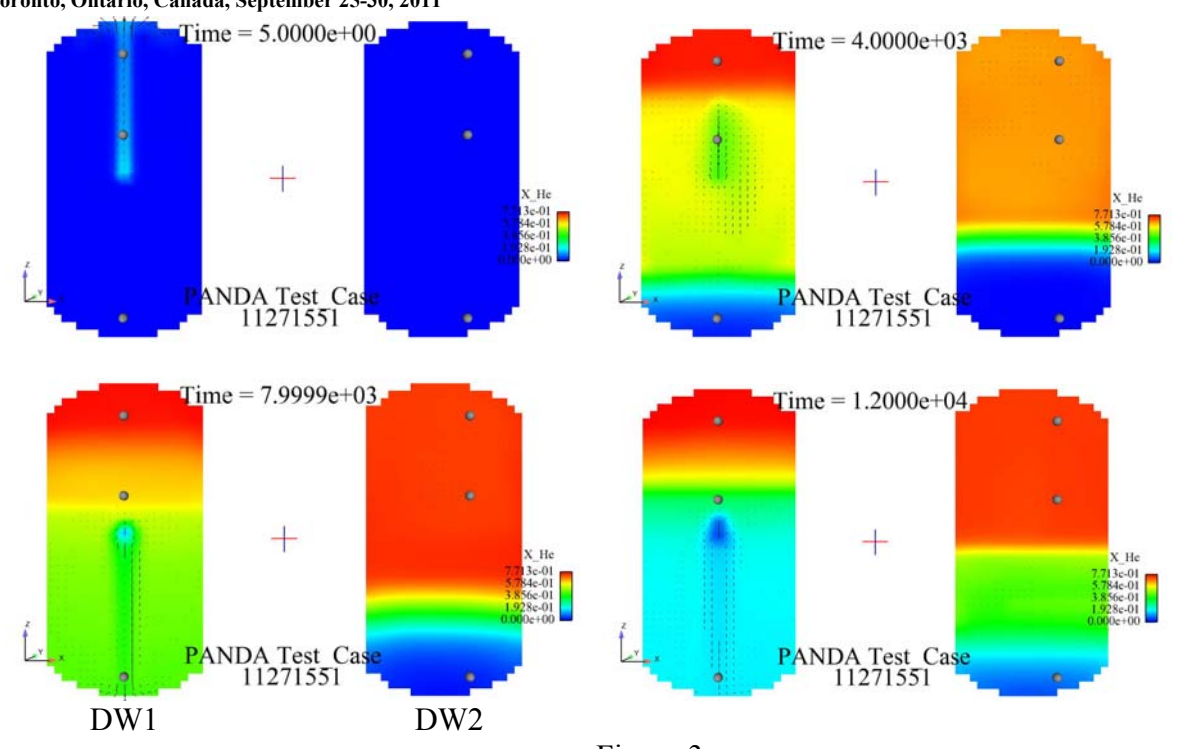
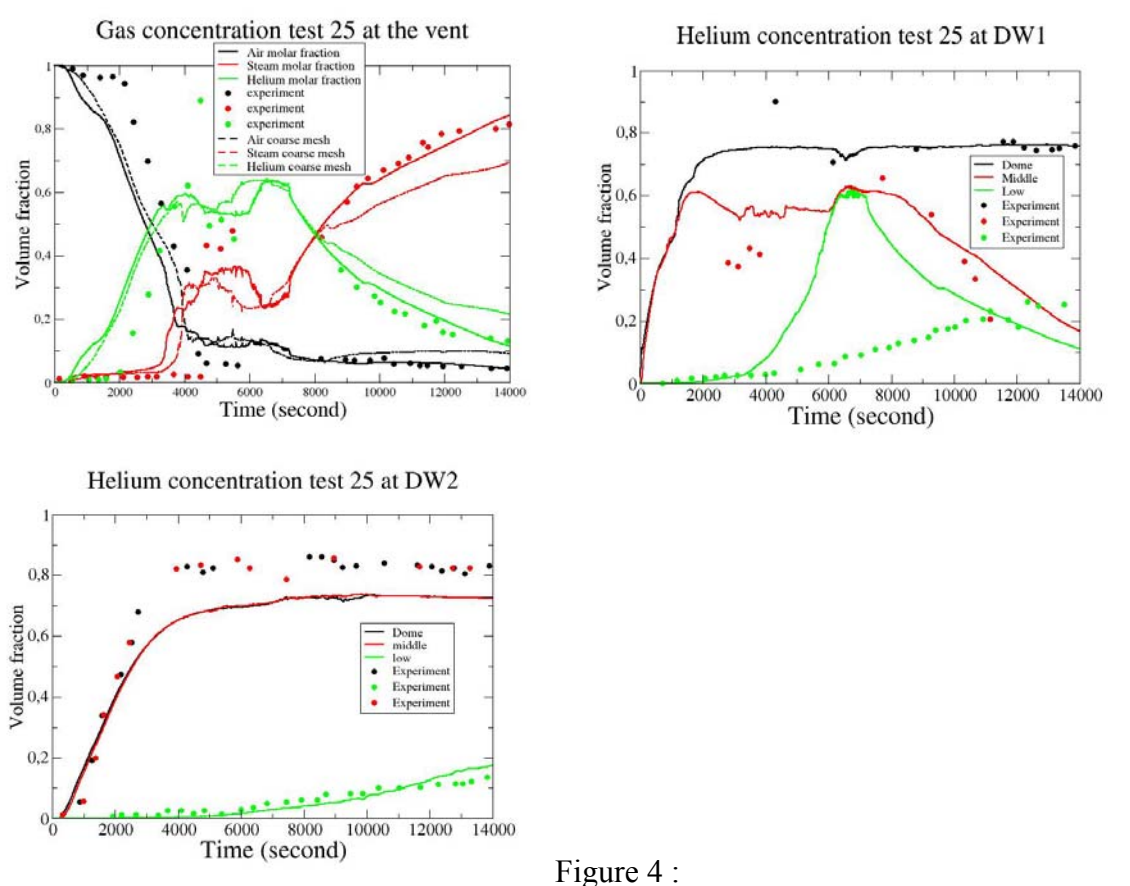


Figure 3
Helium molar fractions in the vertical plane of DW1 and DW2
Positions four times 5, 4000, 8000 and 12000 seconds



Gas volume concentration (Air, Steam, Helium) at the vent and at 3 heights in DW1 and DW2 vessels

The 14th International Topical Meeting on Nuclear Reactor Thermalhydraulics, NURETH-14 Toronto, Ontario, Canada, September 25-30, 2011

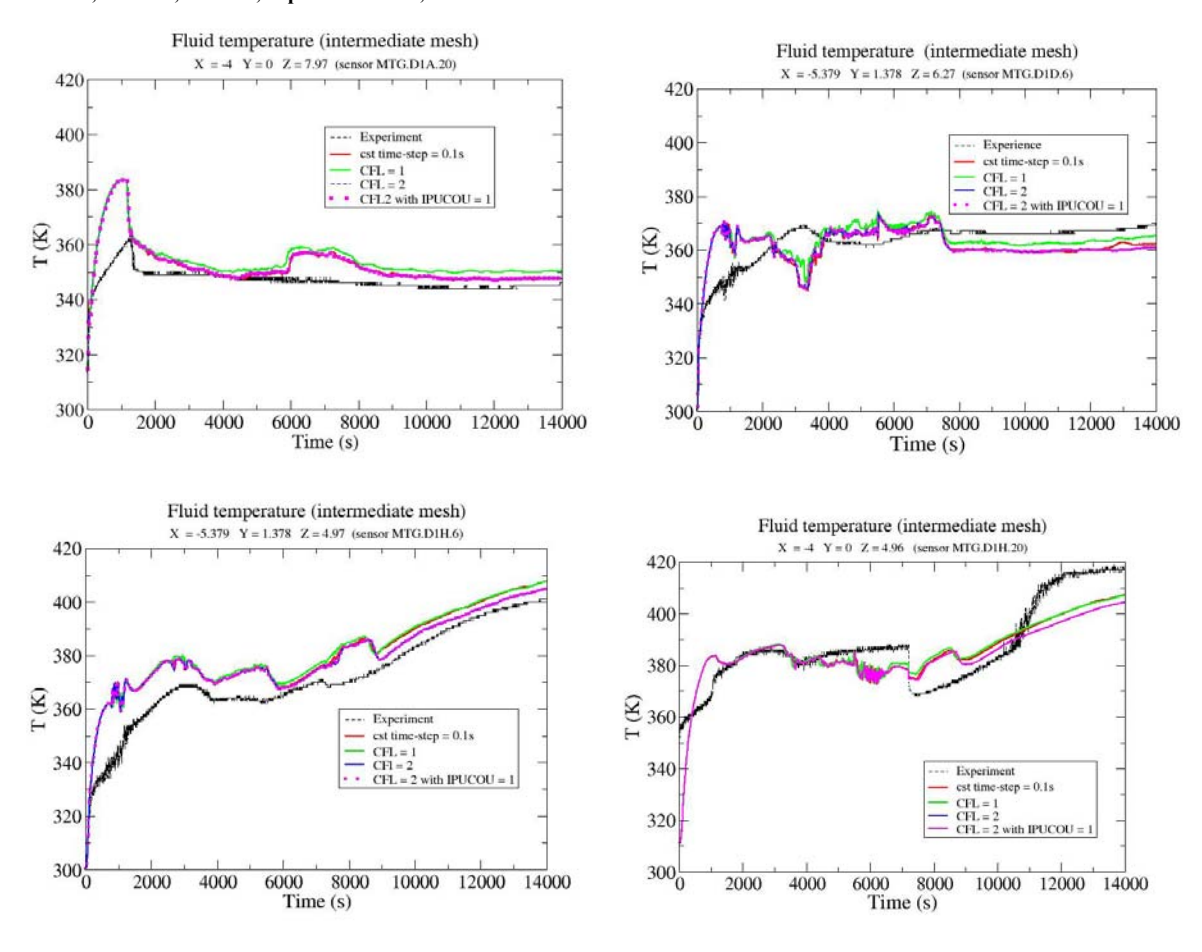
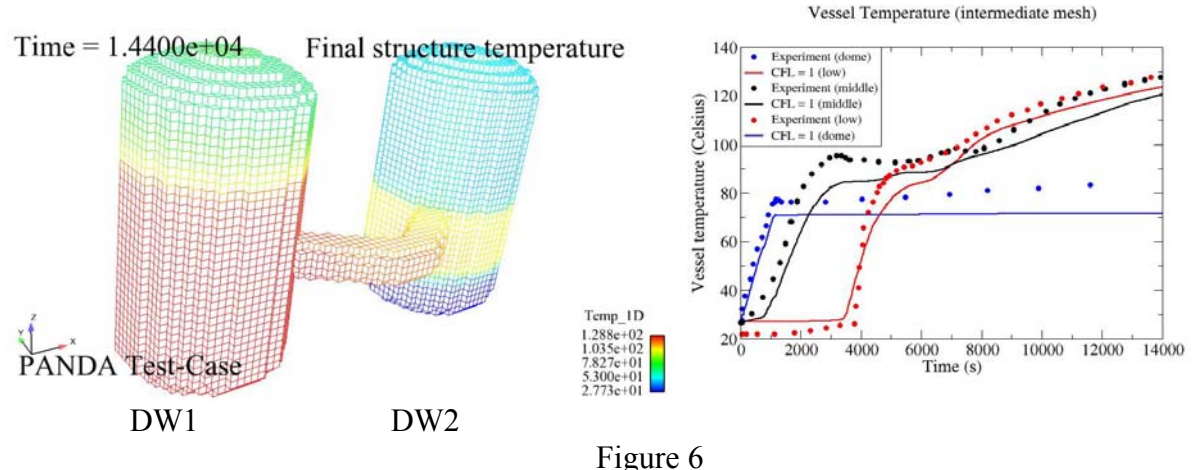


Figure 5
Fluid temperature at 4 locations in DW1 vessel (dome, slightly ex-centered near the dome, ex-centered 1 m above inlet, centered 1 m above the inlet)



Internal structure temperature at final time 14,400 seconds Comparison with experimental data in DW1 at 3 levels (dome, intermediate, low)

3. Conclusion

A large amount of steam and Hydrogen gas is expected to be released within the dry containment of a pressurized water reactor (PWR), after the beginning of a severe accident leading to the melting of the core. The accurate modeling of the gas distribution in a PWR containment concerns phenomena such as wall condensation, hydrogen accumulation, gas stratification and transport in the different compartments of the containment. The paper presents numerical assessments of CFD solver *Code_Saturne* using a simplified homogeneous approach. It is focused on the analysis and the understanding of gas stratification and transport phenomena in compartments.

The numerical simulations are compared with experimental data corresponding to the test 25 of the PANDA experiment. This test concerns the distribution of a mixture of Helium (replacing hydrogen) and steam in air in two vertical and cylindrical vessels, interconnected by a horizontal and cylindrical pipe. The overall dimensions of the experiment (Diameter~4 m, Height~8 m, Volume of the 2 vessels~180 m³) are not yet representative of the true scale of the reactors, but they already provide valuable information when compared to smaller scales (as experience TOSQAN~7m³). The obtained computational results compare fairly well with experimental data and computational results obtained with other codes. The formation of high concentration helium layers in the two vessels is well predicted, as well as the earlier arrival of helium with respect to steam at the vent. The analysis of the different fields (velocity, concentrations, density) and their comparisons with experimental data permit to explain the observed stratifications and to understand the formation of the complex flow structures. Ongoing works concern numerical simulation of PANDA test case 25 with NEPTUNE_CFD, using a multiphase approach for the modeling of condensation (in the fluid and on the walls) and the mechanical drift between steam and liquid water.

The analysis and the comparison of the numerical results with the PANDA database, greatly enriched during the OECD-SETH projects, remain to be done.

Acknowledgments

The work presented here has been achieved in the framework of the EDF R&D project "PAGODES" (Projet Accidents Graves et Outils DE Simulation), dedicated to the PWR severe accidents modeling. The authors are grateful to the signatory partners of the OECD-SETH project funding the PANDA experiments at PSI (Zurich).

4. References

- [1] N. Mechitoua, S. Mimouni, M. Ouraou, E. Moreau, "CFD Modeling of the test 25 of the PANDA experiment". <u>CFD4NRS-3</u>, September 14-16 2010, Washington DC, USA
- [2] F. Archambeau, N. Méchitoua, M. Sakiz, *Code_Saturne*: "a FV code for the computation of turbulent incompressible flows industrial applications", *International Journal of Finite Volume*, Vol. 1 (2004). http://www.latp.univ-mrs.fr/IJFV.
- [3] N. Mechitoua, M. Boucker, J. Lavieville, J.M. Herard, S. Pigny, G. Serre, "An Unstructured Finite Volume Solver for 2-Phase Water/Vapor Flows Modelling Based on an Elliptic Oriented Fractional Step Method", <u>NURETH 10</u>, Seoul, South Korea, October 5-9, 2003.

- [4] A. Guelfi, D. Bestion, M. Boucker, P. Boudier, P. Fillion, M. Grandotto, J-M. Hérard, E. Hervieu, P. Péturaud, "NEPTUNE A new software platform for advanced nuclear thermal hydraulics", *Nuclear Science and Engineering*, vol. 156, pp. 281-324, 2007.
- [5] S. Mimouni, M. Boucker, J. Laviéville, A. Guelfi, D. Bestion, "Modeling and computation of cavitation and boiling bubbly flows with the NEPTUNE_CFD code", *Nuclear. Engineering. And Design* 238 (2008) pp 680-692.
- [6] S. Mimouni J-S. Lamy, J. Lavieville, S. Guieu, M. Martin, Modeling of sprays in containment applications with a CMFD code, *Nuclear Engineering And Design*, in press, available online 21 december 2009.
- [7] S. Mimouni, A. Foissac, J. Lavieville, "CFD modeling of wall steam condensation by a two-phase flow approach", *Nuclear Engineering And Design*, 2010, accepted.
- [8] F. de Cachard, D. Paladino, R. Zboray, M. Andreani, Large scale experimental investigation of gas mixing and stratification in LWR reactors. *Internal final report of Paul Scherrer Institute*, TM-42-07-04, 2007
- [9] F.A. Williams, Combustion Theory, second edition, *Benjamin/ Cummings Publishing Company Inc*, 1985, ISBN 0-8053-9801
- [10] S. Kudriakov, F. Dabbene, E. Studer, A. Beccantini, J.P. Magnaud, H. Paillère, A. Bentaib, A. Bleyer, J. Malet, and C. Caroli, "The TONUS CFD Code for hydrogen risk analysis: physical models numerical schemes and validation matrix", XCFD4NRS-1, Garching (Munich, 2006).
- [11] B.E. Launder, "Turbulence transport models for numerical computation of complex turbulent flows." *Von Karman Institute for fluid dynamics, lecture series 3, 1980*
- [12] A. Murty Kanury, "Introduction to Combustion Phenomena", Combustion Science and Technology Book Series, ISBN 0-677-02690-, 1975
- [13] B. Sapa, L. Gay, N. Méchitoua, P. Plion, H. El Rabii, H.Y. Wang. "URANS approach for buoyancy dominated turbulent diffusion flames." 6th Meditteranean Symposium on Combustion, Ajaccio, France, June 7-11, 2009
- [14] C.M. Rhie, W.L. Chow. A Numerical Study of the Turbulent Flow Past an Isolated Airfoil with Trailing Edge Separation. *AIAA Journal*, vol. 21, pp 1525-1532 (1983)
- [15] P. Royl, J.R. Travis, W. Breitung, Gasflow "Validation with PANDA tests from the OECD SETH Benchmark covering steam/air and steam/helium/air mixtures". *Journal of Science and Technology of Nuclear Installations* special issue IPASS 2008
- [16] D. Paladino, R. Zboray, P. Benz, M. Andreani, "Three Gas Mixture Plume inducing Mixing and Stratification in a multi-compartment containment". <u>NURETH 12</u>, Pittsburgh, Pennsylvania, USA, September 30- October 4, 2007